Journal of Thermal Analysis and Calorimetry
https://doi.org/10.1007/s10973-023-12789-8

Investigation of both thermal parameters and applications of closed-cell plastic thermal insulation foams with building energetic aspects

Ákos Lakatos[1] · Máté Csontos[1] · Attila Csík[2]

Received: 9 August 2023 / Accepted: 24 November 2023

Abstract
Nowadays, if one wants to renovate or build a building, the question of thermal insulation is an essential construction process. Polyurethane is a key thermal insulation material that belongs to plastic foams. It can be applied as a spread or board heat-insulating material. Its thermal insulation properties are superior compared to polystyrene, but still a bit neglected. In this article, we would like to perform thermal investigations executed on a new type of polymeric foam such as polyisocyanurate. We will present acceptably low thermal conductivity (~ 0.022 W m^{-1} k^{-1}), raised specific heat capacity (~ 1400 J kg^{-1} K^{-1}) and calorimetric (bomb and differential) measurement results completed with optical microscopic images. Moreover, scanning electron microscopic analysis and X-ray diffractometry will be also presented. The results will be used for cost calculations applied by buildings and will show justified reasons for its application based on structural measurements too. The results are extremely encouraging.

Keywords PIR · Thermal conductivity · Microscopy · Specific heat capacity and calorimetry

Introduction

In 2022, rising energy (gas, electricity) prices drew everyone's attention to the fact that energy sources should not be wasted. Energy save has become the most important part of countries' energy policies, and it will be even more important in the future. This is also because energy has become a decisive factor in the social and economic development of societies, and energy consumption is increasing rapidly, due to the growing population, urbanization, migration to large cities, and the improvement of living standards [1, 2]. Due to limited energy resources, rapid energy consumption and environmental pollution resulting from the use of fuels, energy save has become mandatory. In many countries, the proportion of energy required for heating buildings is the highest, around 40% in the residential sector [3, 4]. The overcrowding, intense urbanization, excessive resource usage, and social disparities are the main causes of the building sector's severe economic, environmental, technical, and social issues, as well as the unprecedented regional and worldwide climate change. The potential answers to these issues and the policies that are adopted will greatly influence the socioeconomic future, the rate of global growth, and the present and future quality of life for several billion people. We believe that the issues covered in the following paragraphs represent the main difficulties and promising future opportunities in the built environment [5, 6]. The energy used for room heating is almost twice as much as all other sources of consumption. Nowadays, thermal insulation plays an increasingly important role, for which an increasingly wide segment of the industry is trying to offer a solution. Thermal insulation materials are products with a porous or hollow structure and low body density made of some natural or artificially produced material [7]. All forms of heat propagation can be observed in the building materials that make up the building structure, and these can be described numerically together with the thermal conductivity factor. During the thermal technical modernization of a building, thermal insulations can be carried out on the floor laid on

✉ Ákos Lakatos
alakatos@eng.unideb.hu

[1] Department of Building Services and Building Engineering, Faculty of Engineering, University of Debrecen, Ótemető Str 2-4, Debrecen 4028, Hungary

[2] HUN-REN Institute for Nuclear Research, Bem tér 18/C, Debrecen 4026, Hungary

Published online: 27 December 2023

the ground, on the attic, along the external walls, and also on the doors and windows. Many thermal insulation materials are available for these, as the ever-increasing environmental awareness has contributed significantly to the development of the industry. As time goes by, the energy requirements become more and more strict, because it is in everyone's interest to minimize the heating energy demand, thus reducing the carbon dioxide emissions that accelerate the process of global warming. In the field of thermal insulation, we strive more and more to achieve the same thermal insulation effect with as few materials as possible, as economically as possible, which is why thermal insulation is a continuously developing sector.

Brief state of the art thermal insulations

The initial natural thermal insulation materials were gradually replaced by fibrous thermal insulation materials and plastic foams. The thermal conductivity (λ, W m^{-1} K^{-1}) coefficient shows how much heat flows through a material with a unit surface and thickness in a unit of time, depending on the temperature measured on the two bordering sides of the material [8–11]. The thermal conductivity of building materials increases linearly as the temperature increases, and when the temperature decreases, the value of the thermal conductivity also decreases. This can be explained by the fact that the movement of the air particles in the material slows down due to the colder environment, so the thermal conductivity of the material decreases. For this reason, the thermal conductivity of all construction materials is given at a given temperature (+ 10 °C). The increased emission of carbon dioxide seriously endangers the Earth's climate conditions, so appropriate heat insulation is of magnificent significance. In order to achieve the new goals in energy saving, new thermal insulation materials appeared on the market, such the aerogels [12–14], vacuum insulation panels [13–16], and closed-cell plastic foam, such as polyisocyanurate (PIR) [17–23]. The effective thermal conductivity of insulation materials has significantly decreased, falling to 0.004–0.014 W m^{-1} K^{-1} as a result of recent advances in high performance thermal insulators based on nanotechnology. The Knudsen effect, which defines the impact of pore size distributions and partial gas pressure in materials on the gaseous heat transfer, is used to achieve the reductions. The thermal insulation materials that are produced have unique qualities that are significant for the building industry and should be taken into account in every project. The next generation of high-performance thermal insulators might be produced with further exploitation and a similar approach to solid conduction [24]. Plastics are excellent heat insulators and foaming them makes them much better. This is commonly put to good use; however, there are some crucial applications where plastic parts with enhanced thermal conductivity are necessary. Due to the limited thermal conductivity, processing speed may also be constrained in terms of heating and cooling rates. Since most mineral fillers have thermal conductivities that are orders of magnitude greater than those of polymers, they improve the conductivity of composite materials. The percolation effect found in electrical conductivity is often not observed since the process of heat conductivity is driven by a material's capacity to conduct phonons (and not electrons) [25]. Polyurethane foam can be used as a thermal insulation board, as well as in the form of dispersed foam. In the construction industry, it can be found in sprayed form as a thermal insulation material (e.g. window frame sealing), and it is also suitable (e.g. for filling the gaps between pipelines and wire penetrations) and is also an essential thermal insulation material in the production of refrigerators. As a thermal insulation board, it can be found mainly as insulation for high roofs, rafters above or between, but is also suitable for thermal insulation of flat roofs, slabs, floors or facades. PIR is polyisocyanurate, closed-cell hard plastic foam, chemically related to polyurethane (PUR) plastic. The PIR is well-known material at the market; however, this material is a rarely used type of insulation. It carries excellent thermal parameters what are comparable to the parameters of the aerogel insulation; moreover, their market price is not as much as the other available insulators.

The main novelties and purposes of the article can be summarized as follows. In this article, a widespread thermal investigation will be given, executed on two PIR samples manufactured by different factories. Experimental outcomes of the specific heat capacities, thermal conductivities, and calorimetric values will be shown; furthermore, we show the morphology of the samples by microscopic examination of the tested material. The measurements will be completed with building energetic calculations. The main aim of this paper is to highlight the outstanding thermal insulation capability of PIR insulations. The measured results are compared with the results belonging to other plastic foam thermal insulations, and we also highlighted the differences. As the novelty, we present the most important thermal parameters of PIR, measured according to standards, and we show pros and cons regarding the measured parameters. Besides the papers in the literature where the authors focus only on the presentation of thermal conductivities and specific heats capacities and neglected the structural basis (see Ref. [17–23]), we present overall thermodynamic measurement results completed with structural parameters supporting each other, to see the applicability limits of the materials globally. It should be emphasized that these parameters are neglected in the datasheet of the manufacturers. All the measured results are faced to face with other insulations collected from the literature. We also present theoretical approach for the thermal conduction through the PIR. We hope that the collection and

presentation of these measurement data in a publication will help the work of the building design engineers in the future.

Materials and methods

The tested polymeric foams

Polyurethane foams (PUR or PIR) are heat-insulating materials belonging to plastic foams, which are made using the polyaddition process. In terms of packaging, they can be used in tablet or dispersed form, the cellular structure of the tablet packaging is closed, while the cellular structure of the dispersed packaging can be both closed and open. Polyurethane is a polyaddition plastic. For its production, di- and polyisocyanates as well as di- and polyols are used, which react with each other, and long polymer chains and polyurethanes are formed, if the reaction also contains water and/or carboxylic acid. The production process begins with storage, and the liquid materials are stored in a stainless steel container, where they are constantly stirred with the help of paddles, thus preserving the liquid consistency of the materials. Depending on the required proportions, the raw material is fed into the heat exchanger using pipelines, where the polymerization process takes place. From the heat exchanger, the liquid material goes into the dosing heads. Since the material is liquid until it solidifies, it sticks strongly, so it is coated on both sides, which can be a film or a glass veil. The cashiering materials run on the conveyor belt under the dosing heads, onto which the polyurethane is blown, which swells due to the carbon dioxide content of the air and begins to foam. The product is also covered with the top layer, and then it goes into a straightener, where its final thickness is adjusted. In the following step, the product reaches its final shape and strength. The last operation is cutting to the desired size and then unit packaging. Both PUR and PIR are made using the same process, and the difference between them only depends on the amount of isocyanate. PUR foam is flammable, its combustion is accompanied by a high smoke load, and the combustion is directed inwards towards the internal parts. When burning, an oxidation graphite layer is formed on the surface of the PIR foam, which does not continue to burn after extinguishing, but merely chars, and thus also prevents the further spread of the burning towards the inner part the burning dies down [20–22]. Polyurethane thermal insulation panels owe their good thermal conductivity and thermal insulation ability to the pentane gas enclosed in the closed cells that make up their structure, as pentane gas has almost twice the thermal insulation capacity of air. Another priority of the closed-cell structure is that despite the moisture load, its water absorption is negligible. Other advantages include shape retention, durability, and resistance to fungi and mould. It keeps its shape for decades and has high mechanical strength. Its important feature is that it has no ozone-damaging effect on the planet, nor does it have any physiological influence on the human body. Its ignition temperature is around 120 °C, its bulk density is between 30 and 100 kg m^{-3}, and its thermal conductivity value is outstandingly better than its peers, approximately 0.022–0.030 W m^{-1} K^{-1}. Its application is the same as that of polyurethane, but it is mainly used as an insulating foam board, but it also exists in dispersed form, which is used to fill air cavities as a thermal insulator. This insulating material is suitable for interior walls where electric cables run, as it has good heat and flame retardant properties, with a melting point of more than 200 °C. Its foam sheets consist of small closed cells containing chlorinated-fluorinated-hydrocarbon gas (HCFC). It has excellent fire retardant properties. Similar to PUR, they are produced by reacting methylene diphenyl diisocyanate (MDI) with polyol compounds. However, polyisocyanurate has a higher MDI concentration in the final product than polyurethane. When storing them, care must be taken to ensure that the boards do not get wet, as moisture can cause the top layer to separate, and the resulting tension can cause the material to deform. In Table 1, the most important thermal parameters of the tested two types of "PIR1" and "PIR2" thermal insulation materials can be found.

Figure 1a and b represents the shoot image of the tested materials. It can be concluded from the images that PIR2 has a smoother surface than PIR1.

Specific heat capacity and thermal conductivity experiments

The specific heat capacities (cp, J kg^{-1} K^{-1}) and the thermal conductivities (λ W m^{-1} K^{-1}) of the materials with 20 cm × 20 cm base area were examined applying a Netzsch Heat Flow Meter 446 S. According to Ref. [20, 21], firstly we measured these two key thermal parameters. Four materials separately were analysed, and the final values were the mean of each measurement rows both for cp and λ. The instrument is calibrated, and the precision of the test results is less than 2%. The instrument is supplied with a Julabo cooler to quickly and reliably achieve thermal steadiness. The equipment works in accordance with ASTM C518, ISO 8301, JIS A1412, DIN EN 12664, and DIN EN 12667

Table 1 Manufacturer's values of the samples

Material constants by manufacturer	PIR1	PIR2
Fire resistance class	E	E
Thermal conductivity at 10 °C / W m^{-1} K^{-1}	0.024	0.022
Compressive strength at 10% strain / kPa	120	100
Declared density / kg m^{-3}	32	30

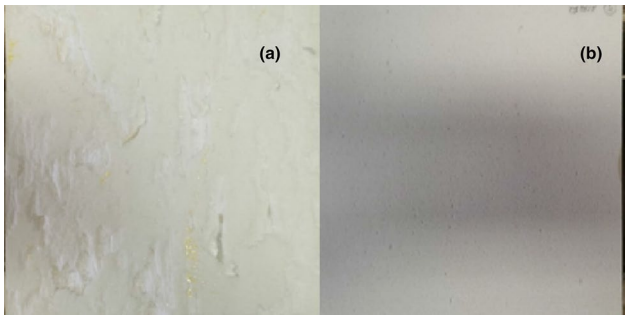

Fig. 1 Photograph image of the tested a) "PIR1" b) PIR2 sample

standards and provides accurate reproducibility [26–28]. This accurate equipment gives an opportunity to precisely estimate the most important thermal parameters of the materials such as the thermal conductivity and specific heat capacity.

Heat flow measurements with DSC

Registering the heat flow in the function of temperature was carried out by a DSC Sirius 3500 instrument from Netzsch. The measurements were executed in nitrogen flow on milled samples with a mass of 5–8 mg placed in an alumina pot from − 20 to 200 °C with a heating rate of 10 K min^{-1} in a double-cycle. The DSC 3500 gives accurate results regarding ISO 11357, ASTM E793, ASTM D3895, ASTM D3418, DIN 51004, DIN 51007, and DIN 53765 standards [28].

Infrared absorption tests

By the method shown in Ref. [29, 30], an infrared absorption test (IR) was also performed. The specimens were positioned together under a Philips shortwave lamp IR with 100 W as a basis, and the temperature on their surface was recorded throughout illumination with a Testo type 868 thermal camera subsequently at 0, 30, 60, and 90 s. Infrared pictures were correspondingly recorded at the same location. This experiment helps to understand the behaviour of materials against direct sunshine. Parallel to this, in every 5 s, the surface temperatures of the irradiated samples were measured with a Testo 905 T2 thermocouple.

Measurement of the gross combustion heat

The gross combustion heat of the samples in pure oxygen gas was measured by cal2 Eco bomb calorimeter. This equipment measures the heat released during the burning of the samples. The heat released is a key point for plastic insulation materials due to their ability for burning. The gross heat of combustion (GCH) of a substance is measured by burning it in a well-ordered, high-purity oxygen gas (30 bar).

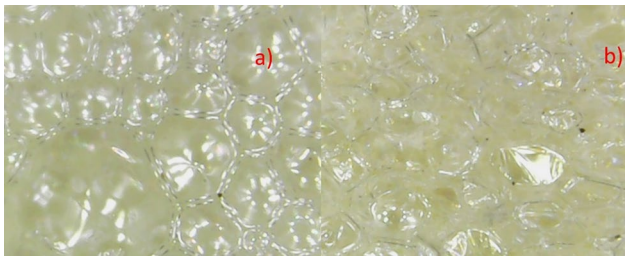

Fig. 2 Optical microscope image of the tested a) "PIR1" and b) PIR2 sample

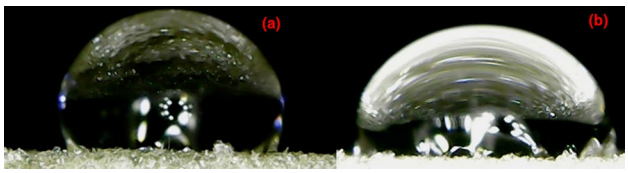

Fig. 3 Hydrophobicity test of the a) "PIR1" sample, with contact angle of 93° and b) "PIR2" sample with 102° contact angle, with less than ± 5% uncertainty

The oxygen bomb calorimeter works as EN ISO 1716 oxygen bomb calorimeter and EN ISO 1182 cylindrical furnace standards.

Results and discussion

Optical microscopic images

The samples were subjected to a microscopic examination, with 40 × magnification to prove the closed-cell, porous structure of the polymer foams, in which the blowing gas with good thermal insulation properties is located. It is a well-known fact about polymers that their surface layers are denser than the inner layers. Closed-cell and rigid PIR foam suffers mechanical damage during its lifetime, during which the outside air can diffuse into the foam cells and the blowing gas diffuses out of them; this process can affect the thermal insulation ability of the foam, as the entering air changes its composition. This phenomenon can cause ageing of the PIR foam, such factors can be solar radiation, temperature, humidity, chemicals, and microorganisms in addition to the ambient air. The closed-cell structure of the materials and the beehive-like arrangement of the cells can be seen in the microscopic image (Fig. 2).

Results of wetting experiments

Figure 3a and b shows the images of the hydrophobic experiments. With the help of microscopic examinations, the hydrophobic properties of the examined PIR foams can

be proven, which means that their surface is water-repellent. We sucked up water with a syringe and then dripped it onto the samples one by one, and the result can be seen when examined from the side with a microscope. From the contact angle of the water droplet with the surface, it can be determined whether the given material is hydrophobic. The contact angle can be measured by placing a drop of liquid on a solid. The angle between the solid/liquid interface is called the contact angle. If the contact angle is greater than 90°, the water droplet is hydrophobic, which means that the material will be water-repellent, it will wet poorly, the adhesion of water droplets will be poor, and the energy content of the solid surface will be low. A droplet with a small contact angle is hydrophilic, which means better wetting ability, adhesion, and higher solid surface energy [31]. The measurements were analysed with ImageJ and CircuDyn softwares.

There has to be mentioned that both EPS and graphite EPS have a higher affinity to take up water due to their open cell structure.

Results of heat capacity (cp) and thermal conductivity (λ) measurements

Both specific heat capacities and thermal conductivities were measured with Netzsch HFM 446 equipment after drying the samples in a Venticell 111 dryer till changeless mass. Four samples from each (PIR1 and PIR2) were tested with 20 cm × 20 cm with 4 cm thickness. The mean value of each measurement resulted in the final values. In the latest papers, the measurement of the key thermal parameters of vacuum insulation panels, aerogels, and graphite EPS materials as advanced insulations was measured with this equipment [28, 32]. In Fig. 4a, we present the thermal conductivities of the two different PIR samples. The measurements were executed between 0 and 50 °C with 10 °C steps and under 20 °C temperature difference. One can see that both curves have a minimum of 10 °C mean temperature. Authors of Ref. [17, 18, 21] found a similar minimum in the thermal conductivity profile.

This minimum is explained by that changes in the thermal conductivity of PIR products are mainly due to changes in the state of blowing gases in the pores due to their diffusion and condensation [17, 18, 21]. One can state that this minimum has the best position in the thermal conductivity vs. temperature curves because the manufacturers should give the declared values of the thermal conductivity of thermal insulation materials. In Fig. 4a, one can see that PIR2 has about 5–6% less thermal conductivity than PIR1. In Table 2, a comparison of the thermal conductivities measured at 10 °C of different frequently used plastic thermal insulations can be found. From Table 2, one can see that both PIR samples have at least 30% less thermal conductivity compared to any EPS insulation. Table 2 also presents thermal conductivities of two types of aerogels. One of them has nearly the same thermal conductivity, while the other one has about 8% less thermal conductivity.

The specific heat capacity in function of temperature at 10, 24 and 40 °C was also measured with the Netzsch HFM 446. The specific heat capacities of both PIR samples are presented in Fig. 4b. It is observable that both samples have a minimum specific heat capacity between 10 and 40 °C by 24 °C. This nonlinear function between the mean temperature and the specific heat capacity was also deduced by the authors of Ref. [21].

They also presented specific heat capacities of EPS samples in this temperature range of around 1200 J kg^{-1} K^{-1}. In a latest paper (Ref. [28]), much less specific heat capacities are presented (800–1200 J kg^{-1} K^{-1}) belonging to graphite EPS and the above-mentioned two aerogel's (slentex, pyrogel).

Differential scanning calorimetry measurements

Heat flow versus temperature curves of milled PIR samples were registered by DSC. Samples were measured with DSC Sirius 3500 equipment from 20 to 200 °C with a heating rate of 10 K min^{-1} in a double heating cycle, under nitrogen flow. The results are presented in Fig. 5a and b. The curves show interesting results. For both samples, a slight peak at about 40 °C, with a glass transition temperature at about 30–35 °C was deduced. Till 200 °C, we did not find a melting effect. The DSC method is suitable for monitoring all processes during which the enthalpy of the system changes. The most important areas of application fall into two large groups that can be classified as: examination of chemical reactions, tracking physical and phase state changes. Glass transition is a typical relaxation transition of amorphous polymers. In the vicinity of the glass transition temperature, the segment movement is released (heating) or frozen (cooling). The same glass transition temperature is found in Ref. [33].

The emergence of a new form of molecular motion or termination of the specific involves a change in heat capacity (cp), which appears as a step on the DSC curve. In most cases, the cp is a stepped change, as well as a local maximum, which can be observed on the DSC curve (peak). Between 10 and 200 °C, we found a change in the specific heat capacity with about 1600 J kg^{-1} K^{-1} for PIR1 and 830 J kg^{-1} K^{-1} for PIR2.

In contrast to the papers published earlier (see Ref. [17–22]) where the focus was only one the measurement of thermal conductivities and specific heat supplied somewhere with DSC measurements, we went further and tried to find a solution for the deviances in the thermal properties (in both λ and cp) between PIR1 and PIR2, and completed our thermal measurements with structural investigations, too. Our goal was to reveal the structural discrepancies between these two

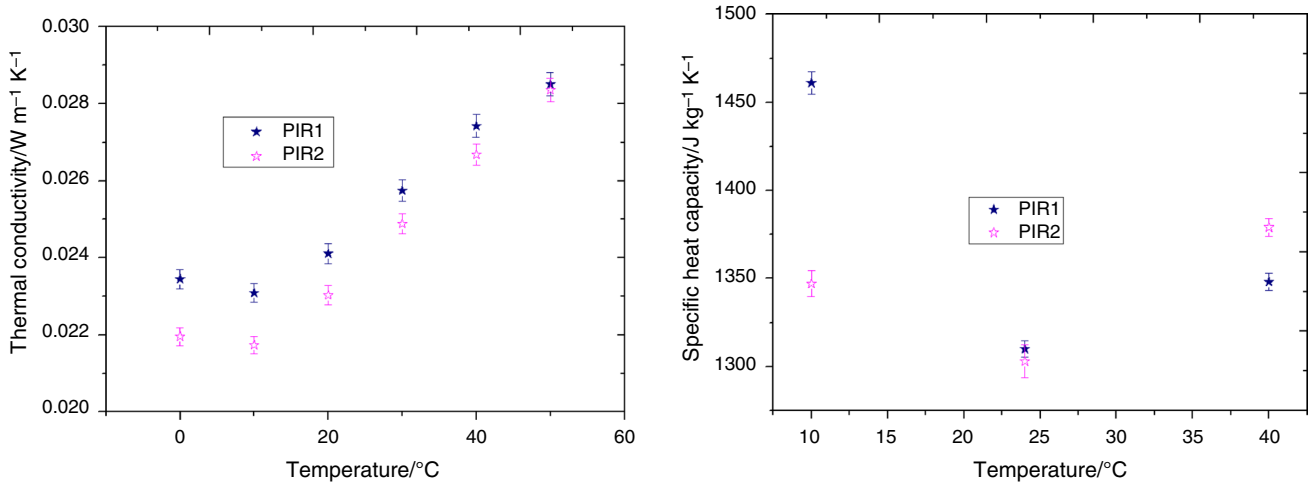

(a) The thermal conductivities of both PIR samples

(b) The specific heat capacities of both PIR samples

Fig. 4 a. Thermal conductivities of both PIR samples. b. The specific heat capacities of both PIR samples

Table 2 Thermal conductivities of various plastic foams at 10 °C

Plastic foam	Thermal conductivity/ W m^{-1} K^{-1}
PIR1	0.023
PIR2	0.022
Graphite EPS	0.031 [28]
Low-density EPS	0.035 [29]
High-density EPS	0.032 [29]
Ultra-high-density EPS	0.03 [29]
Pyrogel aerogel	0.021 [28]
Slentex aerogel	0.0185 [28]

materials as the reason between the difference in the thermal conductivity and in the specific heat capacity as well as in the heat flow curve.

Infrared absorption tests

Thermal insulation materials during the implementation can suffer intensive light irradiation due to direct sunshine. As the rules presented in Ref. [28–30, 34], samples of PIR1 and PIR2 with about 10 cm × 10 cm base area were subjected to IR radiation with a Philips lamp with 100 W power. Parallel to them, a pure white EPS and a graphite EPS were also tested. The measurement order is also presented in Fig. 6a. Before ($t = 0$ s) and during the illumination, thermal images were taken from all samples after 30, 60 and 90 s with a Testo 868 thermo-camera. At the same time, the surface temperature of the samples was also measured every 5 s with a thermocouple. The results are presented in Fig. 6b.

Figure 6a also presents the temperature profiles of the samples. It has to be mentioned that the less surface temperature belongs to the white EPS with about 30 °C surface temperature, while after the illumination for 90 s, graphite EPS reached about 70 °C. It has to be mentioned that the final surface temperature for PIR1 and PIR2 was about 40 °C. It is also presented in Ref. [34] that graphite EPS has a very high thermal absorption ability. In Fig. 6b, one can see the increasing temperature for all samples till 60 s. It has to be mentioned that the signs of M1, M2, M3 and M4 present the measurement point of the temperature. Moreover, in Ref.35, the measurements were also executed for two types of aerogels where the final results after irradiation were in accordance with the results of PIR1 and PIR2.

Measurement of the heat of combustion

The gross combustion heat was measured by Cal2 oxygen bomb calorimeter. The heat released give information about the fire resistance of the insulation material, and it also provides information on how it participates in the spread of the fire. Four combustion heat measurement was executed on PIR1 and PIR2, and the average of the results was compared with the values in the literature [35, 36]. From Table 3, one can see that among the common polymeric insulations, PIR1 and PIR2 have less combustion heat. It means that these materials are also combustible and take part in fire; in addition, the released heat is less during its burning. These results are very important from applicability limit point of view. Based on measurement presented earlier and compared to the ones measured during this case, the PIRs have about a half of combustion heat. This value is excellent among the other combustible plastic insulations.

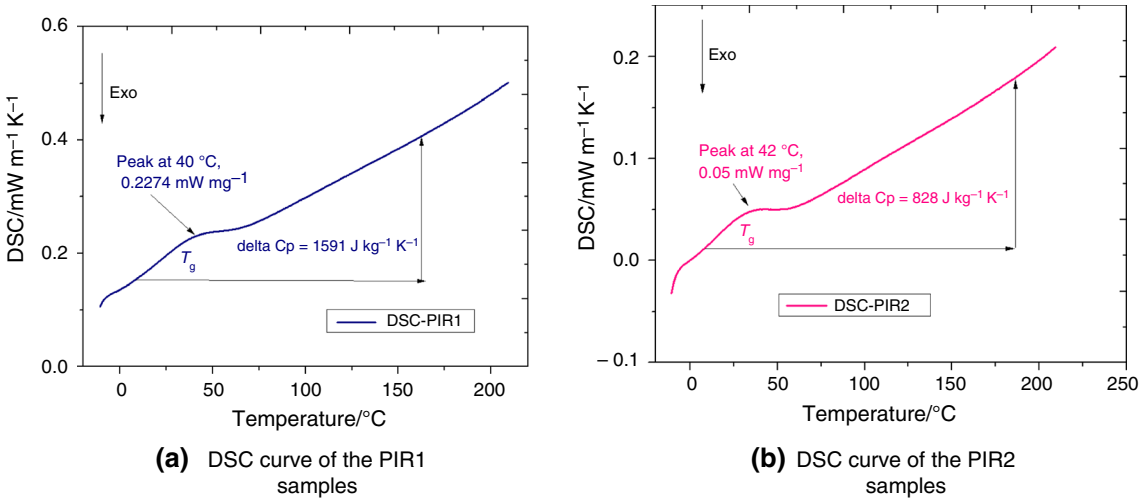

Fig. 5 a. DSC curve of the PIR1 samples. b. DSC curve of the PIR2 samples

Thermal conductivity versus cell size

Figure 7 explains the thermal transmittance through cellular thermal insulation. It is said that the thermal conductivity of cellular insulation can be written by four terms: the conduction through the solid skeleton (red), the thermal conductivity of the gas through collision (blue circles in pair), the thermal convection (blue arrows), and the radiation (orange) [37–42]. By decreasing the cell size, both the thermal conductivity of the gas and the thermal convection of the gas particles can be reduced, since the overall thermal conductivity will be smaller [28]. This can be the interpretation for the smaller (in our case the better) thermal conductivity belonging to PIR2 because the average diameter of the cells of PIR2 is smaller than the value of PIR1. In a smaller cell gas particles, these are expected (see Fig. 7).

Study of structure morphology by scanning electron microscopy

To obtain the size of the cells of the samples, scanning electron microscope (SEM) examinations were executed. A dual beam microscope-type Thermo Fisher Scientific-Scios 2 (FIB-SEM, Waltham, MA, USA) was used to examine the samples. Figure 8a and b presents the SEM images of PIR1 and PIR2 samples, respectively. Different magnifications and 2 kV were used to find the cell diameters. For PIR 1, we reached about 320 µm mean diameter, while the size of the cells of PIR2 was about 260 µm. Authors of Ref. [43] present cell diameters in similar ranges (250–350 µm), for different types of PIRs. Moreover, Ref. [33] presents cell diameters for graphite EPS with about 400–450 µm. The above-mentioned thermal conductivity model is also shown in Fig. 8a and b (left down corner). Figure 8b shows smaller cell diameters with less gas particles (less conduction and convection of molecules) compared to Fig. 8a.

Moreover, Fig. 9 presents the contaminants measured by energy dispersive X-ray spectroscopy (EDS) method. (A Bruker-type detector has been applied in the microscope.)

The results show that the main contaminants are the same for the materials. The slight difference possibly originates from the difference in their manufacturing because they come from two different manufacturers.

Results of X-ray diffractometry experiments

To visualize the amorphous structure of the samples, X-ray diffractometry experiments were executed too by Rigaku SmartLab diffractometer using CuK-alpha irradiation with a wavelength of $\alpha = 0.154$ nm. Bragg–Brentano focusing geometry was applied to scan the samples in 10-80° theta–2theta range.

Figure 10 presents the amorphous peak of the neat PIR samples. Both samples has the same amorphous structure, which is a structural characteristic of a good insulator. A slight different might arise from the above-mentioned difference in the manufacturing processes. This amorphous peak was also presented in Ref. [43, 44].

Applications of the thermal conductivities for a model house, cost calculation

The building on which we conducted the investigation is a newly built single-family house in the inner district of the capital of Hungary (Budapest), during the construction of which it is suggested that the necessary facade thermal insulation will be made of PIR material if it proves to be effective in terms of costs because it has a chance in terms of the

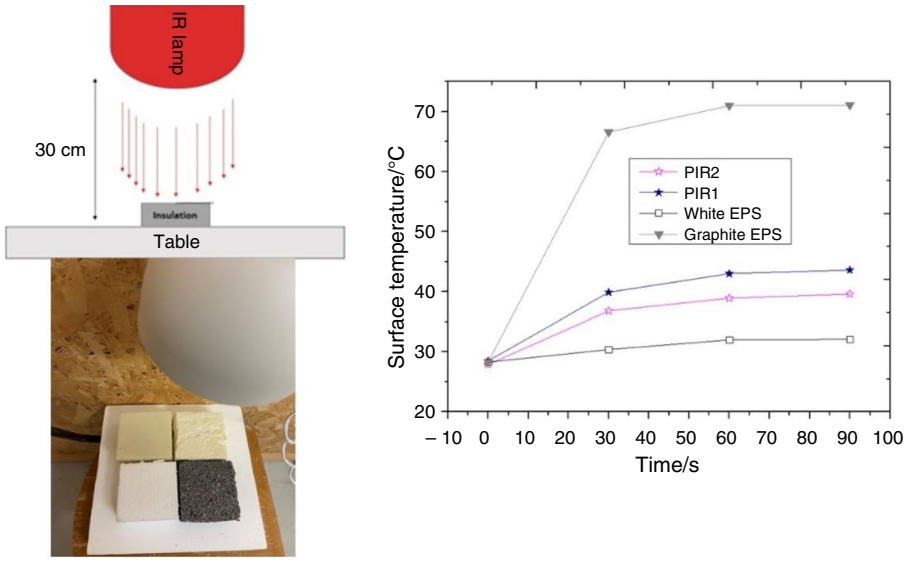

(a) A schematic figure of the infrared absorption test measurement configuration and surface temperature changes during the experiment.

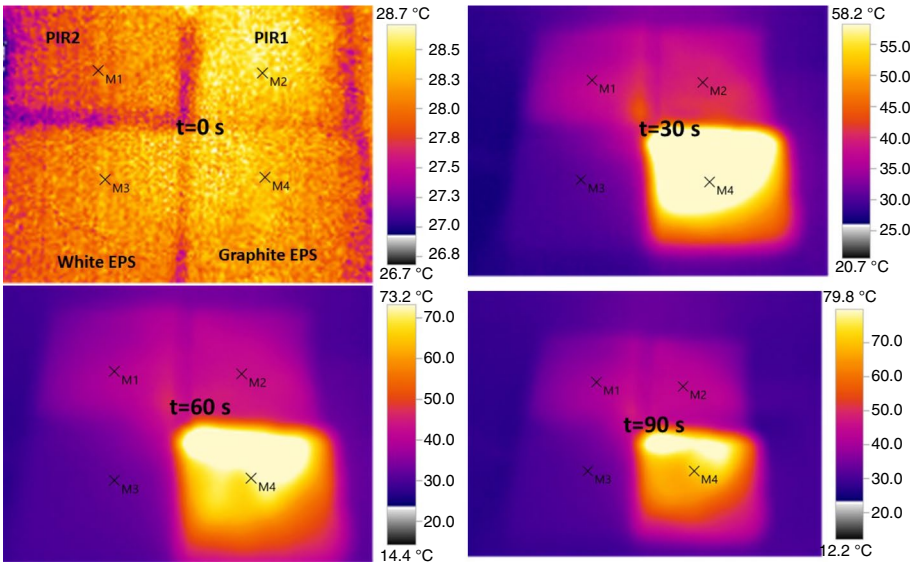

(b) The thermal images of the IR test .

Fig. 6 a. A schematic figure of the infrared absorption test measurement configuration and surface temperature changes during the experiment. b. The thermal images of the IR test

Table 3 Gross combustion heat of both tested PIR1 and PIR2 samples and some other plastic insulation foams from the literature

Samples	Gross combustion heat/ Mj kg^{-1}
PIR1	26.8 ± 0.28
PIR2	27.4 ± 0.75
EPS [31]	45
XPS [47]	40
Graphite EPS [34]	35

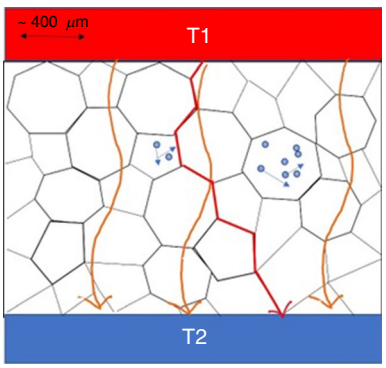

Fig. 7 Thermal transmittance through a cellular insulation

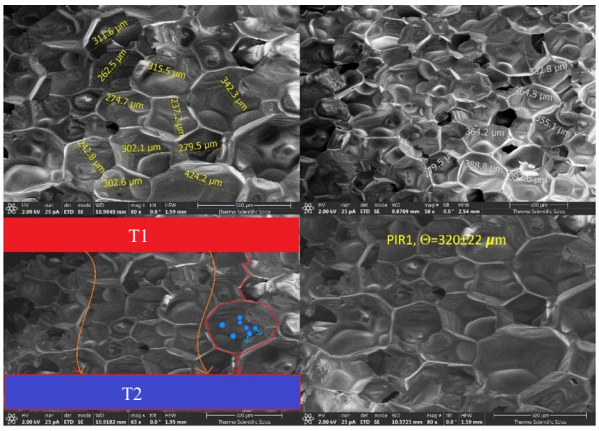

(a) Scanning electron microscopy images of PIR1sample.

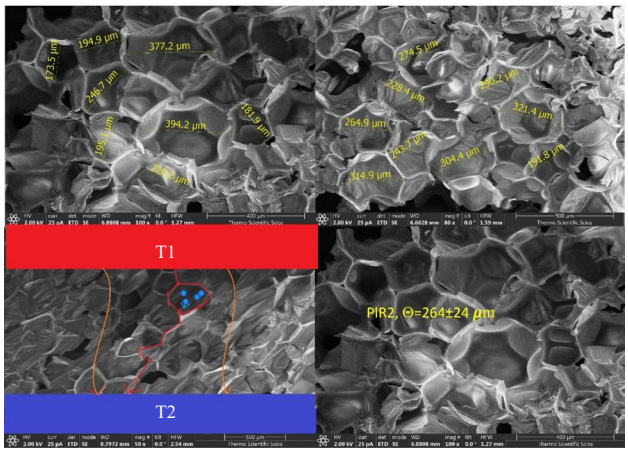

(b) Stucture morphology of the sample PIR2taken by Scanning Electron Microscopy.

Fig. 8 a. Scanning electron microscopy images of PIR1 sample. b. Structure morphology of the sample PIR2 taken by scanning electron microscopy

value of a lower heat conduction factor. That less thickness is sufficient than polystyrene, and thus we can gain valuable saleable space inside the building. We compared how much it would cost to insulate the house with polystyrene and PIR material, and how much area we could save by doing so. In this case, the question is the size of the area that can be saved. We only examined the outer wall layering of the building in the two cases. Regarding Ref. [45], we fixed the overall heat transfer coefficient of the external wall to $U = 0.24$ W m^{-2} K^{-1}. The base wall was a porotherm N + F brick wall with 30 cm thickness. The wall was also covered by plaster both inside and outside. We have calculated the necessary thickness of the insulation to be used for the brick wall to reach the $U = 0.24$ W m^{-2} K^{-1} regulation.

For calculating the U-value (m^2 K W^{-1}), the following equation is used [45, 46]:

$$U = 1/((1/\alpha_i) + \sum (d/\lambda) + (1/\alpha_e)) \quad (1)$$

where α_i and $/\alpha_e$ are the surface heat transfer coefficients 8 and 24, respectively.

If we consider the area to be insulated to 150 m^2, then from the calculations, we deduced that to meet the required U-value, 12 cm from the EPS is necessary, while from the PIR insulation, 6 cm is necessary. In the case that the PIR material is chosen, an area of 3.384 m^2 will be saved. The average square meter price of apartments in the inner districts of Budapest is around 3200 euros. In the case of our apartment, our internal area will be larger by 3.384 m^2, without taking any area from the external area, so the area gained inside can increase the value by approximately 10,000 euros the value of the apartment. The net present values for the establishment (NPV) were found 2400 euros and 3300 euros for the EPS and PIR, respectively. This also pays back if thermal insulation is more expensive with PIR material. Moreover, their price is also much less than both aerogels and vacuum insulation panels.

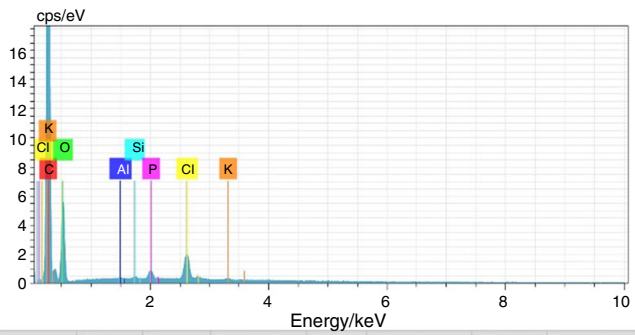

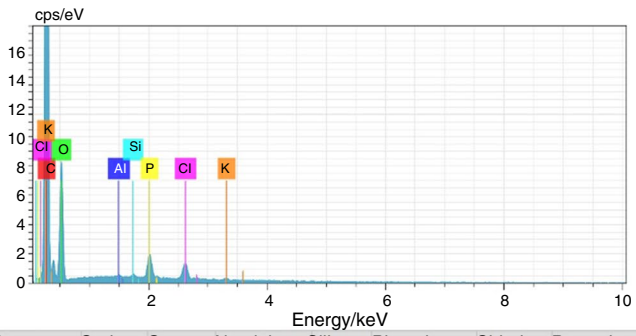

Spectrum	Carbon	Oxygen	Aluminium	Silicon	Phosphorus	Chlorine	Potassium
PIR1	85.30	12.96	0.02	0.08	0.34	1.19	0.10

Spectrum	Carbon	Oxygen	Aluminium	Silicon	Phosphorus	Chlorine	Potassium
PIR2	85.11	13.51	0.05	0.08	0.68	0.53	0.05

Fig. 9 Composition of both samples measured by energy dispersive X-ray spectroscopy (EDS) method

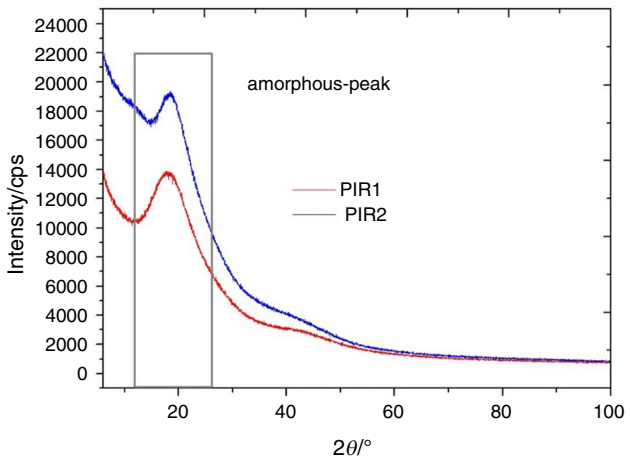

Fig. 10 Results of X-ray diffractometry experiment

Conclusions

As the main aim, of this paper results of an extensive investigation are presented, executed on two types of polyisocyanurate (PIR) samples. During the discussion, we made a complex comparison of the results with available data belonging to different commonly used plastic insulation foams (EPS, graphite EPS) as well as for aerogels. From the results, the following conclusions can be drawn:

- It was stated from microscopic images that both PIR samples have closed beehive-like cell structures with hydrophobic properties (contact angle > 90°).
- From thermal conductivity measurements, we stated that the thermal conductivity versus temperature graph has a minimum (0.022–0.023 W m^{-1} K^{-1}) of 10 °C between 0 and 50 °C; moreover, PIR samples have at least 30% less thermal conductivity compared to any EPS insulation, and their thermal conductivity is in accordance with aerogel slabs.
- Specific heat capacity results indicated higher heat storage capacity from the PIR insulations compared to EPS and aerogel samples, with a value of 1300–1500 J kg^{-1} K^{-1} in the temperature range of 10–40 °C.
- Differential scanning calorimetry results indicated the thermal stability of the PIR samples between 0 and 200 °C, without melting, and only dehydration was detected.
- From the results of IR absorption tests, we proved that PIR samples have a much less infrared absorption rate compared to graphite EPS, and after 90 s of irradiation, the surface of the PIR reached about 40 °C, while graphite EPS had 70 °C.
- After characterization of the gross combustion heat of PIR samples, we pointed out that PIR is also a combustive material, but it has less involvement in spreading the fire compared to EPS samples, and we found about 27 MJ kg^{-1} for the GHC, while the polystyrene derivatives had more than 35 MJ kg^{-1}.
- X-ray diffractometry proved the amorphous structure of the samples.
- SEM images presented smaller cell sizes for PIR2. This result proved the less thermal conductivity of PIR2. As a basis, we presented a new theory improvement for the thermal conductivity of cellular insulations.
- From building energetic calculations, we also stated that PIR has relevance in application as structural thermal insulation. It has a slightly higher price than the EPS, but has much more thermal insulation capability and can save the area from the construction site.

Acknowledgements Project no. TKP2021-NKTA-34 has been implemented with the support provided by the Ministry of Innovation and Technology of Hungary from the National Research, Development and Innovation Fund, financed under the TKP2021-NKTA funding scheme.

Author contributions Conceptualization and supervision were done by ÁL. Data curation was done by ÁL and MC. Funding acquisition was done by ÁL. Methodology was done by ÁL. Writing—original draft preparation was done by ÁL, MC, and AC. Writing—review and editing was done by ÁL, MC, and AC. Investigation was done by ÁL, MC, and AC. Measurements were taken by ÁL, MC, and AC (SEM, XRD). Project administration was done by ÁL.

Funding Open access funding provided by University of Debrecen.

Declarations

Competing interest The authors declare that they have no known competing financial interests/personal relationships that could have appeared to influence the work reported in this paper.

References

1. Berardi U. A cross-country comparison of the building Energy consumptions and their trends. Resour Conserv Recycl. 2017;123:230–41. https://doi.org/10.1016/j.resconrec.2016.03.014.
2. Hámori S, Kalmár F. Hydraulic balancing analysis of a central heating system with constant supply temperature. EEMJ. 2014;13(11):2789–95.

3. Zhang L, Yuan J, Kim CS. Application of energy-saving building's designing methods in marine cities. Energy Rep. 2023;9(Supplement 8):98–110.
4. Kashan ME, Fung AS, Eisapour AH. Insulated concrete form foundation wall as solar thermal energy storage for cold-climate building heating system. Energy Convers Manag X. 2023;19:100391. https://doi.org/10.1016/j.ecmx.2023.100391.
5. Santamouris M, Vasilakopoulou K. Present and future energy consumption of buildings: challenges and opportunities towards decarbonisation. e-Prime Adv Electr Eng Electron Energy. 2021;1:100002.
6. Csanády D, Fenyvesi O, Nagy B. An empirical model of heat-treated straw bulks' thermal conductivity based on changes in mass and chemical composition. J Therm Anal Calorim. 2023;148:3731–49. https://doi.org/10.1007/s10973-023-11945-4.
7. Abdul-Zahra AS, Al Jubori AM. Potential evaluation and analysis of near-to-net zero energy building in hot and dry climate. Energy Convers Manag X. 2021;12:100146. https://doi.org/10.1016/j.ecmx.2021.100146.
8. Khoukhi M, Hassan A, Al Saadi S, Abdelbaqi S. A dynamic thermal response on thermal conductivity at different temperature and moisture levels of EPS insulation. Case Stud Therm Eng. 2019;14:100481. https://doi.org/10.1016/j.csite.2019.100481.
9. Cai S, Zhang B, Cremaschi L. Review of moisture behavior and thermal performance of polystyrene insulation in building applications. Build Environ. 2017;123:50–65. https://doi.org/10.1016/j.buildenv.2017.06.034.
10. Cai S, Xia L, Xu H, Li X, Liu Z, Cremaschi L. Effect of internal structure on dynamically coupled heat and moisture transfer in closed-cell thermal insulation. Int J Heat Mass Transf. 2022;185:122391. https://doi.org/10.1016/j.ijheatmasstransfer.2021.122391.
11. Tran MP, Gong P, Detrembleur C, Thomassin JM, Buahom P, Saniei M, Kenig S, Parka CB, Lee SE. Reducing thermal conductivity of polymeric foams with high volume expansion made from polystyrene/expanded graphite. SPE ANTE, 1870–1882; 2016
12. Yildiz A, Ali Ersöz M. Determination of the economical optimum insulation thickness for VRF (variable refrigerant flow) systems. Energy. 2015;89:835–44.
13. Ni L, Luo Y, Qiu C, Shen L, Zou H, Liang M, Liu P, Zhou S. Mechanically flexible polyimide foams with different chain structures for high temperature thermal insulation purposes. Mater Today Phys. 2022;26:100720.
14. Liu H, Liu J, Tian Y, Wu X, Li Z. Investigation of high temperature thermal insulation performance of fiber-reinforced silica aerogel composites. Int J Therm Sci. 2023;183:107827.
15. Alam M, Singh H, Limbachiya MC. Vacuum insulation panels (VIPs) for building construction industry–a review of the contemporary developments and future directions. Appl Energy. 2011;88:3592–602.
16. Sprengard C, Holm AH. The thermal bridging effects are only reduced by covering layers made of insulating materials on the surfaces of the VIP. Energy Build. 2014;85:638–43.
17. Makaveckas T, Bliūdžius R, Burlingis A. Determination of the impact of environmental temperature on the thermal conductivity of polyisocyanurate (PIR) foam products. J Build Eng. 2021;41:102447. https://doi.org/10.1016/j.jobe.2021.102447.
18. Zhang H, Fang WZ, Li YM, Tao WQ. Experimental study of the thermal conductivity of polyurethane foams. Appl Therm Eng. 2017;115:528–38.
19. Liszkowska J, Czupryński B, Paciorek-Sadowska J. Thermal properties of polyurethane-polyisocyanurate (PUR-PIR) foams modified with tris(5-hydroxypenthyl) citrate. J Adv Chem Eng. 2016;6:2. https://doi.org/10.4172/2090-4568.1000148.
20. Berardi U, Madzarevic J. Microstructural analysis and blowing agent concentration in aged polyurethane and polyisocyanurate foams. Appl Therm Eng. 2020. https://doi.org/10.1016/j.applthermaleng.2019.114440.
21. Yousefi Y, Tariku F. Thermal conductivity and specific heat capacity temperatures. J Phys Conf Ser. 2021;2069:012090.
22. Gravit M, Kuleshin A, Khametgalieva E, Karakozova I. Technical characteristics of rigid sprayed PUR and PIR foams used in construction industry. IOP Conf Ser Earth Environ Sci. 2017;90:012187.
23. Molleti S, Van Reenen D. Effect of temperature on long-term thermal conductivity of closed-cell insulation materials. Buildings. 2022;12:425.
24. Rothon R, DeArmitt C, in Brydson's Plastics Materials (Eighth Edition), 2017, 8.6.4.8.1 Conductivity
25. Baetens R, in Nanotechnology in Eco-Efficient Construction, 2013
26. ISO 8301:1991, Thermal insulation—Determination of steady-state thermal resistance and related properties—Heat flow meter apparatus
27. EN ISO 10456:2007. Building materials and products. Hygrothermal properties. Tabulated design values and procedures for determining declared and design thermal values. ISO: Geneva; 2007
28. Lakatos Á. Thermal insulation capability of nanostructured insulations and their combination as hybrid insulation systems. Case Stud Therm Eng. 2023;41:102630.
29. Pan J, Chen F, Cabrera DE, Min Z, Ruan S, Wu M, Zhang D, Castro JM, Lee JL. Carbon particulate and controlled-hydrolysis assisted extrusion foaming of semicrystalline polyethylene terephthalate for the enhanced thermal insulation property. J Cell Plast. 2021;57:695–716. https://doi.org/10.1177/0021955X20952751.
30. Pan J, Zhang D, Wu M, Ruan S, Castro JM, Lee JL, Chen F. Impacts of carbonaceous particulates on extrudate semicrystalline polyethylene terephthalate foams: nonisothermal crystallization, rheology, and infrared attenuation studies. Ind Eng Chem Res. 2020;59:15586–97.
31. Novak V, Zach J. Study of the efficiency and durability of hydrophobization modifications of building elements. IOP Conf Ser Mater Sci Eng. 2019;583:012032.
32. Lakatos Á, Kovács Z. Comparison of thermal insulation performance of vacuum insulation panels with EPS protection layers measured with different methods. Energy Build. 2021;236:110771.
33. Hou R, Zhang Z, Zhang G, Tang D. Synthesis and properties of thermoplastic polyisocyanurates: polyisocyanuratoamide, polyisocyanurato(ester-amide) and polyisocyanurato (urea-ester). J Renew Mater. 2020;8(4):397–403.
34. Lakatos Á, Csík A. Multiscale thermal investigations of graphite doped polystyrene thermal insulation. Polymers. 2022;14(8):1606. https://doi.org/10.3390/polym14081606.
35. Fangrat J. On non-combustibility of commercial building materials. Fire Mater. 2017;41:99–110. https://doi.org/10.1002/fam.2369.
36. Lakatos Á, Deák I, Berardi U. Thermal characterization of different graphite polystyrene. Int Rev Appl Sci Eng. 2018;9(2):163–8. https://doi.org/10.1556/1848.2018.9.2.12.
37. Liu H, Tian Y, Jiao J, Wu X, Li Z. Thermal conductivity modeling of hollow fiber-based porous structures for thermal insulation applications. J Non-Cryst Solids. 2022;575:121188.
38. Kovács Z, Szanyi S, Budai I, Lakatos Á. Laboratory tests of high-performance thermal insulations. In: Littlewood J, Howlett R, Capozzoli A, Jain L, editors. Sustainability in energy and buildings. Smart innovation, systems and technologies, vol. 163. Singapore: Springer; 2020. https://doi.org/10.1007/978-981-32-9868-2_7.
39. Zhao K, Ye F, Cheng L, Yang J, Chen X. An overview of ultra-high temperature ceramic for thermal insulation: structure and

composition design with thermal conductivity regulation. J Eur Ceram Soc. 2023;43(16):7241–62.
40. Jelle BP, Gustavsen A, Baetens R. The path to the high performance thermal building insulation materials and solutions of tomorrow. J Build Phys. 2010;34(2):99–123.
41. Jelle BP, Tilset BG, Gao T, Grandcloas M, Lovvik OM, Bohne RA, Mofid AS, Ng S, Sagvolden E. High-performance nano insulation materials for energy-efficient buildings. In: Proceedings of TechConnect World Innovation Conference 2017, pp. 289–292, Washington DC, 2017; Washington DC
42. Lakatos Á. Thermal conductivity of insulations approached from a new aspect. J Therm Anal Calorim. 2018;133(1):329–35.
43. Lazo M, Puga I, Macías MA, Barragán A, Manzano P, Rivas A, Rigail-Cedeño A. Mechanical and thermal properties of polyisocyanurate rigid foams reinforced with agricultural waste. Case Stud Chem Environ Eng. 2023;8:100392. https://doi.org/10.1016/j.cscee.2023.100392.
44. Leng W, Li J, Cai Z. Synthesis and characterization of cellulose nanofibril-reinforced polyurethane foam. Polymers. 2017;9(11):597. https://doi.org/10.3390/polym9110597.
45. Nardi I, Lucchi E. In situ thermal transmittance assessment of the building envelope: practical advice and outlooks for standard and innovative procedures. Energies. 2023;16:3319. https://doi.org/10.3390/en16083319.
46. /2006 TNM, ministerial decree without portfolio
47. Khoukhi M, Hassan A, Al Saadi S, Abdelbaqi S. A dynamic thermal response on thermal conductivity at different temperature and moisture levels of EPS insulation. Case Stud Therm Eng. 2019;14:100481.
48. Capozzoli A, Fantucci S, Favoino F, Perino M. Vacuum insulation panels: analysis of the thermal performance of both single panel and multilayer boards. Energies. 2015;8:2528–47.
49. Kreativlakas.com, [Online]. Available: https://kreativlakas.com/hoszigetelo-anyagok/poliuretan-hab-gyartasa-tulajdonsagai-es-felhasznalasa/. Accessed 25 Oct 2022.
50. Lakatos Á. Measurements of thermal properties of different building materials. Adv Mater Res. 2014;1016:733–7.